

# Statistical mechanical approach of complex networks with weighted links

Rute Oliveira,<sup>1</sup> Samurá Brito,<sup>2,3</sup> Luciano R. da Silva,<sup>1,4</sup> and Constantino Tsallis<sup>4,5,6,7</sup>

<sup>1</sup>Federal University of Rio Grande do Norte, Departamento de Física Teórica e Experimental, Natal-RN, 59078-900, Brazil.

<sup>2</sup>Emerging Technology Group at Itau-Unibanco

<sup>3</sup>International Institute of Physics, Federal University of Rio Grande do Norte, 59070-405 Natal, Brazil

<sup>4</sup>National Institute of Science and Technology of Complex Systems, Brazil.

<sup>5</sup>Centro Brasileiro de Pesquisas Físicas, Rua Xavier Sigaud 150, 22290-180 Rio de Janeiro-RJ, Brazil.

<sup>6</sup>Santa Fe Institute, 1399 Hyde Park Road, New Mexico 87501, USA

<sup>7</sup>Complexity Science Hub Vienna, Josefstädter Strasse 39, A 1080 Vienna, Austria.

(Dated: May 17, 2022)

Systems which consist of many localized constituents interacting with each other can be represented by complex networks. Consistently, network science has become highly popular in vast fields focusing on natural, artificial and social systems. We numerically analyze the growth of  $d$ -dimensional geographic networks (characterized by the index  $\alpha_G \geq 0$ ;  $d = 1, 2, 3, 4$ ) whose links are weighted through a predefined random probability distribution, namely  $P(w) \propto e^{-|w-w_c|/\tau}$ ,  $w$  being the weight ( $w_c \geq 0$ ;  $\tau > 0$ ). In this model, each site has an evolving degree  $k_i$  and a local energy  $\varepsilon_i \equiv \sum_{j=1}^{k_i} w_{ij}/2$  ( $i = 1, 2, \dots, N$ ) that depend on the weights of the links connected to it. Each newly arriving site links to one of the pre-existing ones through preferential attachment given by the probability  $\Pi_{ij} \propto \varepsilon_i/d_{ij}^{\alpha_A}$  ( $\alpha_A \geq 0$ ), where  $d_{ij}$  is the Euclidean distance between the sites. Short- and long-range interactions respectively correspond to  $\alpha_A/d > 1$  and  $0 \leq \alpha_A/d \leq 1$ ;  $\alpha_A/d \rightarrow \infty$  corresponds to interactions between close neighbors, and  $\alpha_A/d \rightarrow 0$  corresponds to infinitely-ranged interactions. The site energy distribution  $p(\varepsilon)$  corresponds to the usual degree distribution  $p(k)$  as the particular instance  $(w_c, \tau) = (1, 0)$ . We numerically verify that the corresponding connectivity distribution  $p(\varepsilon)$  converges, when  $\alpha_A/d \rightarrow \infty$ , to the weight distribution  $P(w)$  for infinitely wide distributions (i.e.,  $\tau \rightarrow \infty$ ,  $\forall w_c$ ) as well as for  $w_c \rightarrow 0$ ,  $\forall \tau$ . Finally, we show that  $p(\varepsilon)$  is well approached by the  $q$ -exponential distribution  $e_q^{-\beta_q|\varepsilon-w'_c|}$  [ $0 \leq w'_c(w_c, \alpha_A/d) \leq w_c$ ] which optimizes the nonadditive entropy  $S_q$  under simple constraints;  $q$  depends only on  $\alpha_A/d$ , thus exhibiting universality.

## I. INTRODUCTION

Network science is extremely effective in studying large interacting systems. Within this approach, systems are described by graphs, with nodes (or sites) representing the individual components and edges (or links) representing the interactions between them. Empirical studies show that complex networks are ubiquitous [1–3]. It has been possible, along such lines, to understand the propagation of information [4, 5], classical and quantum internet connections [6, 7], scientific collaborations [8, 9], epidemiology [10, 11], and human brain [12]. Consistently, in recent decades, mathematical models have emerged to mimic real systems and reproduce their structural properties [13]. In Euclidean space, geographical networks have also been studied, such as subway systems [14], neural [15], internet and transportation networks [16]. Also, many real world networks are weighted by assigning real numbers to their edges [17, 18]. For example, the US air transportation network [19], where the weights of the edges represent the total number of passengers.

Statistical mechanics is intensively used to study systems with complex geometric and topological properties. In many such systems, the elements exhibit long-range interactions [20]. To handle these cases, a generalization of the Boltzmann–Gibbs (BG) statistical mechanics was proposed in 1988 [21], currently referred to as nonextensive statistical mechanics, based on the nonadditive entropies  $S_q = k \frac{1 - \sum_i p_i^q}{q-1}$  with  $q \in \mathbb{R}$ . The BG theory is recovered for  $q \rightarrow 1$ . This generalized approach has been applied in a large variety of systems, e.g., spin-glasses [22], astrophysical plasma [23], urban agglomerations [24], velocities of collective migrating cells [25], cold atoms in dissipative optical lattices [26, 27], among others.

The relationship between asymptotically scale-free  $d$ -dimensional geographic networks and nonextensive statistical mechanics started being explored in 2005 [28–33], where a preferential attachment index  $\alpha_A$  and a growth index  $\alpha_G$  were included. These studies showed that geographic networks exhibit three regimes: (a)  $0 \leq \alpha_A/d \leq 1$ , corresponding to strongly long-range interactions, (b)  $1 \leq \alpha_A/d \lesssim 5$ , corresponding to moderately long-range interactions, and (c)  $\alpha_A/d \gtrsim 5$ , corresponding to the BG-like regime, i.e.,  $q \simeq 1$  (short-range interactions).

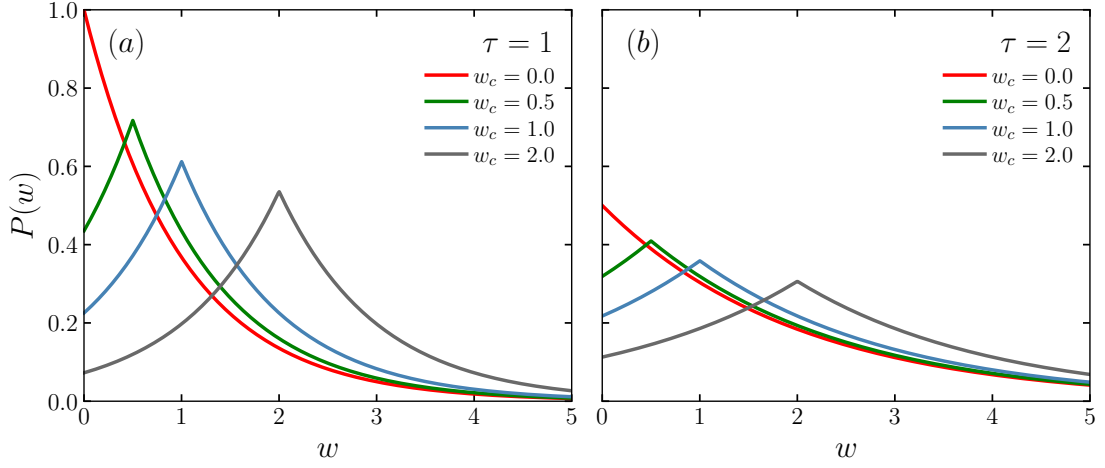


FIG. 1. Examples of weight distributions  $P(w) \propto e^{-|w-w_c|/\tau}$  used for the network links. This distribution is defined within the range  $w \in [0, \infty)$  which characterizes an asymmetric Laplace-like distribution with the free parameters  $w_c \geq 0$  and  $\tau > 0$  that control the location of the peak and its width (scale parameter) respectively. Its special case  $w_c = 0$  corresponds to the exponential distribution. (a)  $P(w)$  for  $\tau = 1$  and typical values of  $w_c = (0, 0.5, 1.0, 2.0)$ . (b) The same as in (a) but with scale parameter  $\tau = 2$ .

In a recent study, we have introduced a  $d$ -dimensional geographical network with weighted links [33] where we use a stretched-exponential distribution  $P(w)$  for the weight  $w$ . We analyzed the distribution of site 'energies' (or costs)  $p(\varepsilon)$ , where

$$\varepsilon_i \equiv \sum_{j=1}^{k_i} \frac{w_{ij}}{2}, \quad (1)$$

$k_i$  being the degree of the  $i$ -th site; the factor  $1/2$  is introduced to avoid double counting between the sites, where only half of the link width is assigned to the site  $i$ . We verified that  $p(\varepsilon)$  is numerically very close to  $p_q(\varepsilon) \equiv e_q^{-\beta_q \varepsilon} / Z_q$ , where  $p_q(\varepsilon)$  generalizes the BG factor,  $\beta_q$  playing the role of an inverse temperature and  $Z_q$  being the normalization factor; the  $q$ -exponential function is defined as  $e_q^z \equiv [1 + (q-1)z]^{\frac{1}{1-q}}$  ( $e_1^z = e^z$ ). We also showed that  $q$  exhibits a universal behaviour, depending only on the scaled variable  $\alpha_A/d$ .

Our aim here is to study the energy distribution  $p(\varepsilon)$  corresponding to a Laplace-like weight distribution. In particular, we compare  $p(\varepsilon)$  with  $P(w)$  and with the  $q$ -exponential form.

The comparison of distributions is common in diverse scenarios. From algorithms to generate pseudo-random numbers [34], through the validity of empirical data with regard to the corresponding theoretical distribution [35, 36] and the identification of images [37, 38], to distributions of aquatic organisms [39]. Interestingly enough, the studies [40, 41] show that the site energy (total weight) distribution converges (excepting for a logarithmic correction) to the scaling behavior of the connectivity (or degree) distribution of the network. Empirical studies exhibit some real-world examples of networks where this phenomenon or similar ones have been observed, e.g., in book borrowing, movie actor collaborations [41], worldwide airport connections, scientific collaborations [42], and others. In the present work we numerically show that, when  $(\tau \rightarrow \infty, \forall w_c)$  and  $(w_c \rightarrow 0, \forall \tau)$ , the energy distribution  $p(\varepsilon)$  and the weight distribution  $P(w)$  become identical in the regime of short-range interactions ( $\alpha_A/d \gg 1$ ).

The paper is structured as follows. In Sec. II we describe our network model, including the weight distribution and its stochastic implementation. In Sec. III we analyze the numerical energy distribution and compare it with the weight distribution of the links, as well as with the  $q$ -exponential form emerging from optimizing the nonadditive entropy  $S_q$ . Finally, in Sec. IV we conclude.

## II. THE MODEL

Our network model starts with one site at the origin and then, for each new site added to the network, we randomly sample a position for it according to the isotropic distribution  $p(r) \propto 1/r^{d+\alpha_G}$  ( $\alpha_G > 0$ ;  $d = 1, 2, 3, 4$ ), where  $r \geq 1$  is the Euclidean distance from the center of mass to the new site, and  $\alpha_G$  is the growth index. Then, we link every newly arriving site ( $j$ ) to one of the pre-existing ones in the network according to the following preferential attachment rule:

$$\Pi_{ij} = \frac{\varepsilon_i d_{ij}^{-\alpha_A}}{\sum_k \varepsilon_k d_{kj}^{-\alpha_A}} \in [0, 1] \quad (\alpha_A \geq 0), \quad (2)$$

where  $d_{ij}$  is the Euclidean distance between sites  $i$  and  $j$  and the attachment index  $\alpha_A$  characterizes the range of the interactions; when  $\alpha_A \rightarrow 0$  the system has long-range interactions and the distance loses relevance, whereas for  $\alpha_A \rightarrow \infty$  the sites have short-range interactions (connections between close neighbors). To each site of the network we associate, through Eq. (1), a local *energy*  $\varepsilon_i$  which depends on the number of links.

In the present paper, we are using the following Laplace-like distribution (see Fig. 1) for the weights of the links:

$$P(w) = \frac{1}{2\tau - \tau e^{-w_c/\tau}} e^{-|w-w_c|/\tau} \quad (w_c \geq 0; \tau > 0), \quad (3)$$

which satisfies  $\int_0^\infty dw P(w) = 1$ ,  $\tau$  characterizing the distribution width and  $w_c$  being the peak location parameter. The parameter  $\tau$  influences the wide of the distribution: when  $\tau \rightarrow 0$  the distribution displays a prominent peak around  $w_c$ , whereas, in contrast,  $\tau \rightarrow \infty$  corresponds to an infinitely wide distribution. To numerically get values of the variable  $w$  from this distribution we use the inverse transformation method [43]:

$$w = w_c - \text{sgn} \left[ u - A\tau(1 - e^{-w_c/\tau}) \right] \tau \ln \left\{ 1 + \text{sgn} \left[ u - A\tau(1 - e^{-w_c/\tau}) \right] \left[ 1 - (u/A\tau + e^{-w_c/\tau}) \right] \right\}, \quad (4)$$

where  $A = 1/(2\tau - \tau e^{-w_c/\tau})$  is the normalization constant [see Eq. (3)],  $u$  is a uniform random variable between  $[0, 1]$  and  $\text{sgn}(\theta)$  denotes the sign function:

$$\text{sgn}(\theta) = \begin{cases} -1, & \text{if } \theta < 0, \\ 0, & \text{if } \theta = 0, \\ 1, & \text{if } \theta > 0. \end{cases}$$

## III. SIMULATIONS AND RESULTS

We now focus on the energy distribution  $p(\varepsilon)$  and compare it with the weight distribution of the links  $P(w)$ . The weight distribution has two free parameters, namely  $\tau$  and  $w_c$ , while our model has three parameters, namely  $\alpha_A$ ,  $\alpha_G$  and  $d$ , in addition to the weight distribution itself. We fix these parameters and numerically determine  $p(\varepsilon)$  by using a large number  $N$  of sites (typically  $N = 10^5$ ) and performing a large number of realizations (typically  $10^3$ ).

We verify that the energy distribution is completely independent from  $\alpha_G$  in all situations, as already discussed in earlier publications [28–31, 33]. Consequently, we fix it to be  $\alpha_G = 1$  in all our simulations. Also, we observe that  $p(\varepsilon)$  remains invariant when we fix  $\alpha_A/d$  and we modify the values of  $d = 1, 2, 3, 4$ , as shown in Fig. 2. This implies an universality property, namely that the energy distribution depends on the ratio  $\alpha_A/d$  and does not depend independently on  $\alpha_A$  and on  $d$  [29–33]. In consequence, we present our results by simply running  $d = 2$ .

We choose typical values for the parameter  $\tau = 1$  and  $10$ , and for the location parameter  $w_c = 0, 0.25, 0.5, 1$  and  $2$ , and generate networks for fixed values of the attachment parameter  $\alpha_A$ . We compare the weight and the energy distributions through their histograms by using a function from the Python Library Numpy [44]. This function has some input parameters (array, bins, density, etc.) and returns the probability density function at each bin (with  $n$  bins in total,  $b_1, \dots, b_n$ ) where the integral over the entire interval equals unity.

There are many methods in the literature for comparing histograms. We use here two of them, namely Histogram Intersection [37] and Q–Q (quantile-quantile) plot, to compare  $p(\varepsilon)$  and  $P(w)$ . The histogram intersection method

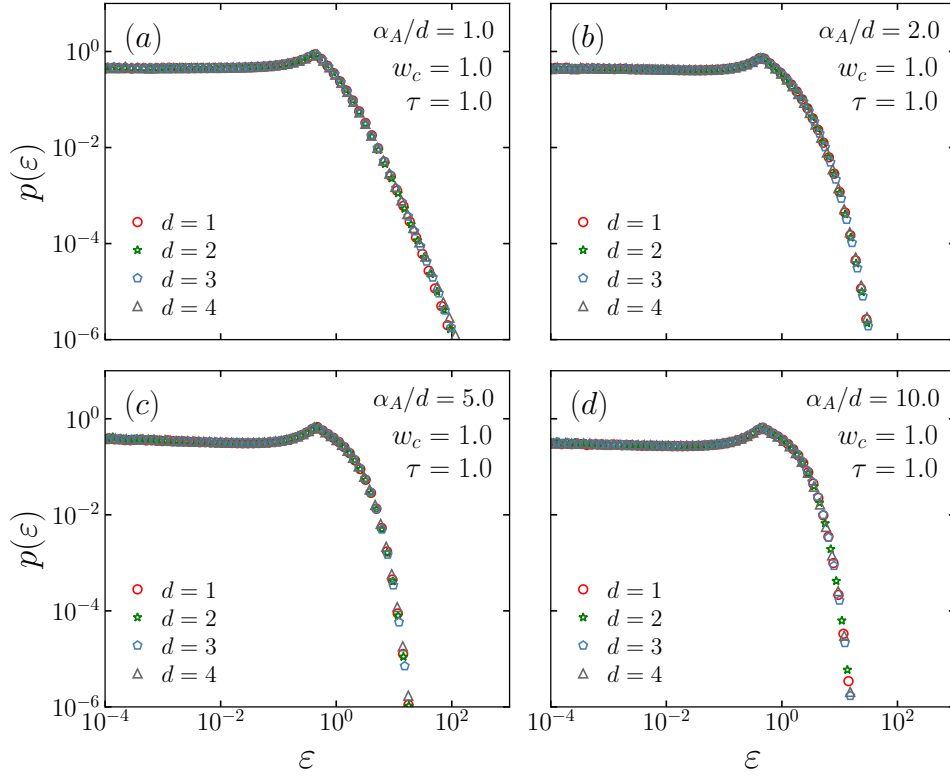


FIG. 2. Local energy distribution  $p(\varepsilon)$  for typical values of  $d = 1, 2, 3, 4$  with (a)  $\alpha_A/d = 1$ , (b)  $\alpha_A/d = 2$ , (c)  $\alpha_A/d = 5$  and (d)  $\alpha_A/d = 10$  by fixing  $(\alpha_G, \tau, w_c) = (1, 1, 1)$ . We verify that, for all values of  $d$ , the curves of  $p(\varepsilon)$  remain invariant, i.e., the dimensionality does not influence the energy distribution. For simplicity, we set  $w_c = \tau = 1$ , but the results remain independent from this choice. The simulations are averaged over  $10^3$  realisations for  $N = 10^5$  sites.

is a technique used for image indexing and comparison, where the image colors are discretized by a histogram and compared to a original figure. Given two histograms,  $H_w$  and  $H_\varepsilon$ , containing the same number  $n$  of bins, Swain and Ballard [37] defined the histogram intersection as the sum of the minima for all histogram bins:

$$H_w \cap H_\varepsilon = \sum_{i=1}^n \min [h_w(i), h_\varepsilon(i)], \quad (5)$$

the range of this calculus goes from 0 to 1, where 0 indicates that the histograms do not intersect at all and 1 means that the histograms are identical.

In Figs. 3 and 4 we show the energy and weight distributions for  $\tau = 1$  and  $\tau = 10$  respectively. We observe that when  $\alpha_A/d \sim 1$  the histograms are sensibly different, whereas when  $\alpha_A/d$  increases they become quite similar. In the limit  $\alpha_A/d \rightarrow \infty$ , the distributions are practically identical. This behaviour is shown in Fig. 5. This result is more pronounced when  $w_c \rightarrow 0$ .

Alternatively, we can also recover the same results through the quantile probability plot (Q-Q plot), which is a graphical method for comparing two probability distributions by plotting the quantile of the first distribution against the same quantile of the second one. If  $F(x)$  is a distribution function, the  $p^{th}$  quantile of  $F$  is defined as [45]:

$$\xi_p \equiv \inf\{x : F(x) \leq p\} \quad (0 < p < 1). \quad (6)$$

If the two distributions are very close, the points in the Q-Q plot will fall approximately along a straight line, namely the bisector. Otherwise, if the points form a nonlinear curve, then the distributions are different. Figure 6 presents a Q-Q plot for the energy of the sites against the weights of the links. We observe that the quantile

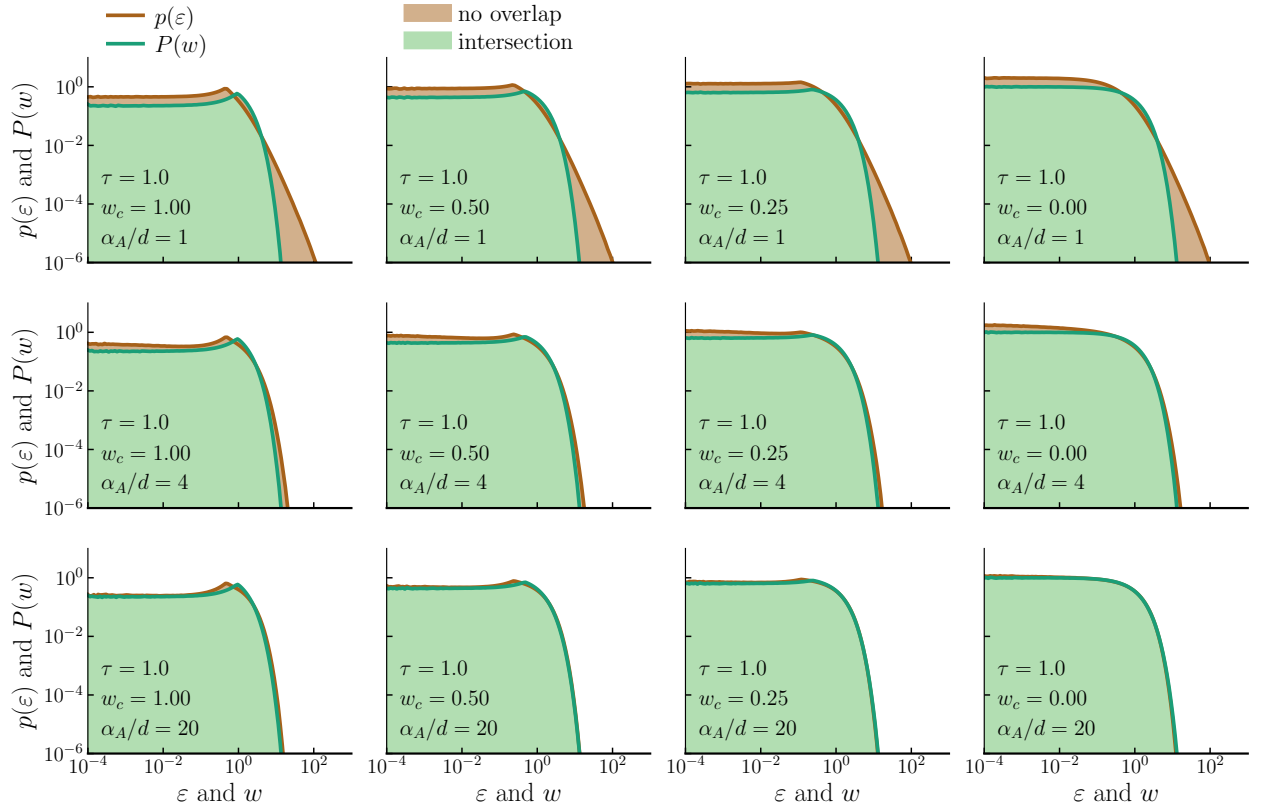


FIG. 3. Comparison between the distribution  $P(w)$  of the associated link weights and the energy distribution  $p(\varepsilon)$  of the network. The green and brown continuous lines respectively represent  $P(w)$ , given by Eq. (3), and  $p(\varepsilon)$ . The green-shaded area is the region of intersection and the brown-shaded area denotes the region where the weight and energy distributions do not intersect. We analyzed a large amount of typical cases with  $w_c = (1, 0.50, 0.25, 0)$  and  $\alpha_A/d = (1, 4, 20)$ , with  $\tau = 1$ . For large values of  $\alpha_A/d$  the results show that the distribution curves are similar in the tail with different peaks where the maximum value of the energy distribution is shifted to the left; if  $w_c \rightarrow 0$  the distributions become identical. The simulations are averaged over  $10^3$  realisations for  $N = 10^5$  sites.

TABLE I. Values used for  $\beta_{q_0}$  and  $\beta_{q_\infty}$  in Eq. (9). The parameters  $\beta_{q_0}$  and  $\beta_{q_\infty}$  correspond to  $\alpha_A/d = 1$  and  $\alpha_A/d = 20$  respectively. These results are for  $N = 10^5$  sites averaged over  $10^3$  realizations.

| $w_c$ | $\beta_{q_0}$ | $\beta_{q_\infty}$ |
|-------|---------------|--------------------|
| 0.00  | 3.33          | 1.14               |
| 0.25  | 2.80          | 1.04               |
| 0.50  | 2.55          | 1.00               |

probability plot accentuates the comparative structure of the tails of the variables  $\varepsilon$  and  $w$ . When  $\alpha_A/d = 1$  the discrepancy between the distributions is clearly evident, where the weight distribution has a considerably shorter tail than the energy distribution.

Let us now compare  $p(\varepsilon)$  with the following  $q$ -exponential form:

$$p_q(\varepsilon) = \frac{e_q^{-\beta_q |\varepsilon - w'_c|}}{Z_q}, \quad (7)$$

where  $w'_c \in [0, w_c]$  is a location parameter playing the role of a chemical potential in  $p_q(\varepsilon)$ ,  $q$  is the entropic index,  $\beta_q$  playing the role of an inverse temperature, and  $Z_q$  is the normalization factor (see Fig. 7a-c); we remind that the weight distribution analysed in the present paper differs from that analysed in [33]. The particular case  $w_c = 0$

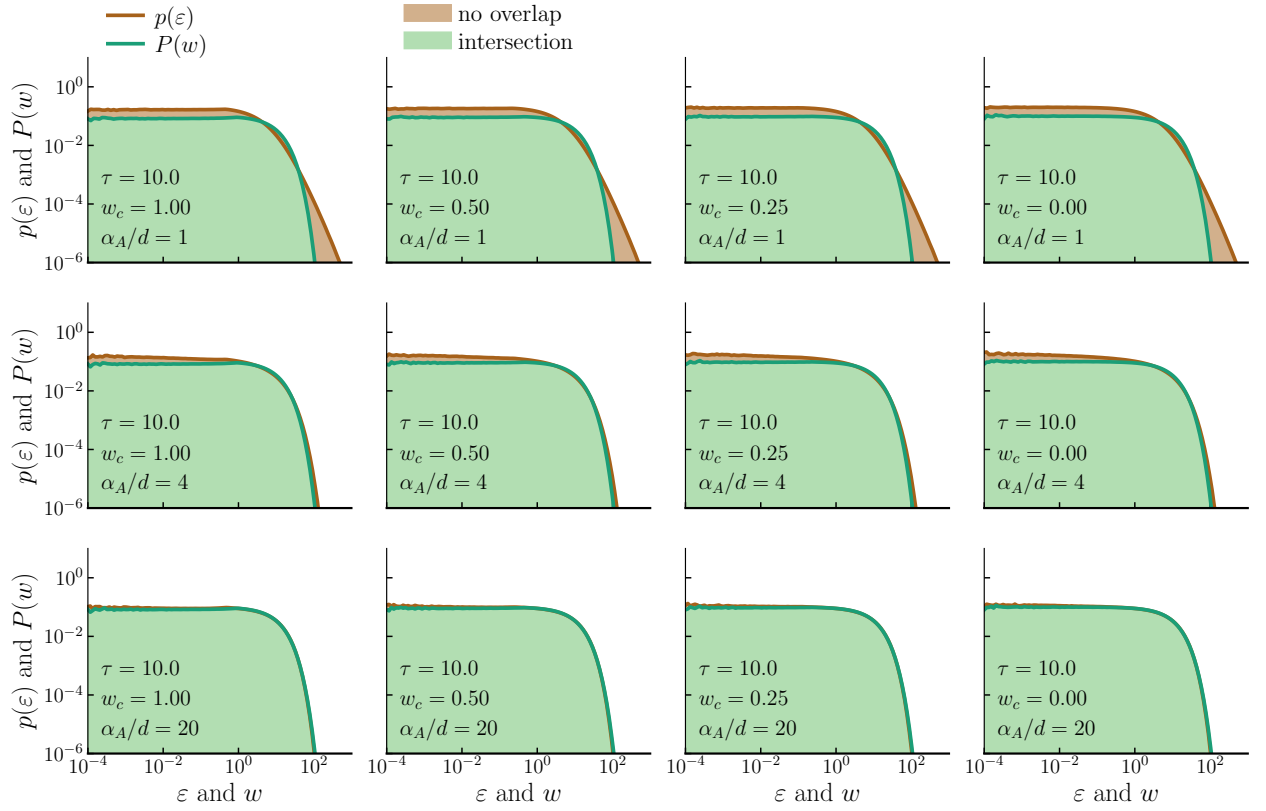


FIG. 4. The same as in Fig. 3 but with  $\tau = 10$ .

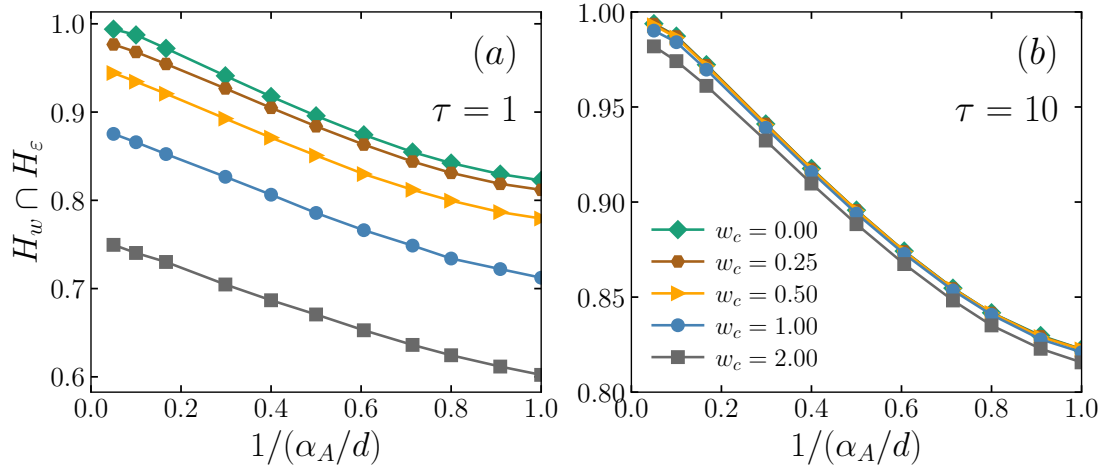


FIG. 5. Intersection between the histogram  $H_\varepsilon$  of site energies and the histogram  $H_w$  of the link weights. Every point was calculated using Eq. (5) for (a)  $\tau = 1$  and (b)  $\tau = 2$ , and typical values of  $w_c = (0, 0.25, 0.5, 1, 2)$ . As we can see in (a), all the curves attain the maximum value at  $\alpha_A/d \rightarrow \infty$ , but only for  $w_c \sim 0$  the intersection between histograms approaches 1, showing that the distributions  $p(\varepsilon)$  and  $P(w)$  are practically identical when  $\tau = 1$ ,  $w_c \sim 0$ . We can observe in (b) that the curves exhibit a maximum close to 1 regardless of the location parameter  $w_c$ . This result is a consequence from the fact that  $P(w)$  becomes an infinitely wide distribution, i.e., when  $\tau \rightarrow \infty$ , and, simultaneously,  $\alpha_A/d \rightarrow \infty$ , i.e., the network exhibits connectivity only between sites that are very close.

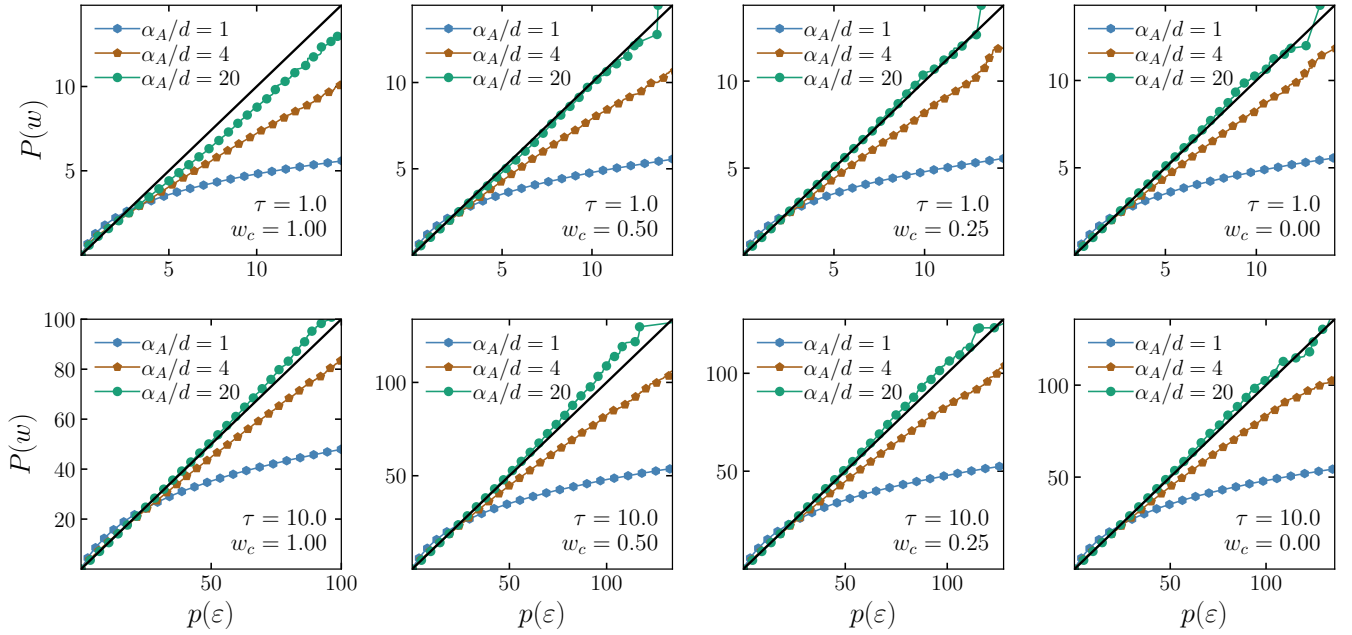


FIG. 6. Q-Q plot for  $\tau = 1$  (top) and  $\tau = 10$  (bottom), and typical values of  $\alpha_A/d = 1$  (blue diamond), 4 (brown hexagon), 20 (green circle). In all cases the black continuous line corresponds to the bisector. The simulations were averaged over 800 realisations for  $N = 10^5$  sites.

corresponds to an exponential distribution and we recover the results obtained in our previous study [33], where we used the stretched-exponential distribution for the link weight  $P(w) \propto e^{-(w/w_0)^\eta}$  for  $\eta = 1$ . Once again, this result exhibits the emergence of an interesting correspondence between a geometrical random network problem and a particular case within nonextensive statistical mechanical systems.

In Fig. 7(d-f) we exhibit the variables  $q$ ,  $\beta_q$  and  $w'_c$  as functions of the ratio  $\alpha_A/d$ . We numerically show that  $q$  only depends on this ratio;  $\beta_q$  also depends on  $w_c$ . Interestingly enough, both variables are given by the same equations indicated in [33], i. e.,

$$q = \begin{cases} \frac{4}{3} & \text{if } 0 \leq \frac{\alpha_A}{d} \leq 1 \\ \frac{1}{3} e^{1-\alpha_A/d} + 1 & \text{if } \frac{\alpha_A}{d} > 1 \end{cases} \quad (8)$$

and

$$\tau\beta_q = \begin{cases} \beta_{q_0} & \text{if } 0 \leq \frac{\alpha_A}{d} \leq 1 \\ (\beta_{q_0} - \beta_{q_\infty}) e^{2(1-\alpha_A/d)} + \beta_{q_\infty} & \text{if } \frac{\alpha_A}{d} > 1, \end{cases} \quad (9)$$

where the variables  $\beta_{q_0}$  and  $\beta_{q_\infty}$  are listed in Table I. This fact was not necessarily expected a priori, and it probably appears because, in both cases, we use  $q$ -exponentials to approach our results. In all cases we observe the existence of three regimes, consistent with [29, 31, 33]. For  $0 \leq \alpha_A/d \leq 1$ ,  $q$ ,  $\beta_q$  and  $w'_c$  are constants, the system presenting very-long-range interactions. For  $1 < \alpha_A/d \lesssim 5$ , the system exhibits moderately-long-range interactions, where  $q$  and  $\beta_q$  monotonically decrease with  $\alpha_A/d$ , whereas  $w'_c$  increases. In the limit of  $\alpha_A/d \rightarrow \infty$ , the parameters tend to constant values and this regime corresponds to short-range interactions ( $q \rightarrow 1$ ).

#### IV. CONCLUSIONS

Many real systems contain sites whose importance (here denoted as *energy*) is generated by interactions with the other sites through weighted links. This is the kind of situation that our network model mimics. Our simulations yield energy distributions which depend on  $\alpha_A$  and on  $d$  through the ratio  $\alpha_A/d$ . Indeed, the results collapse

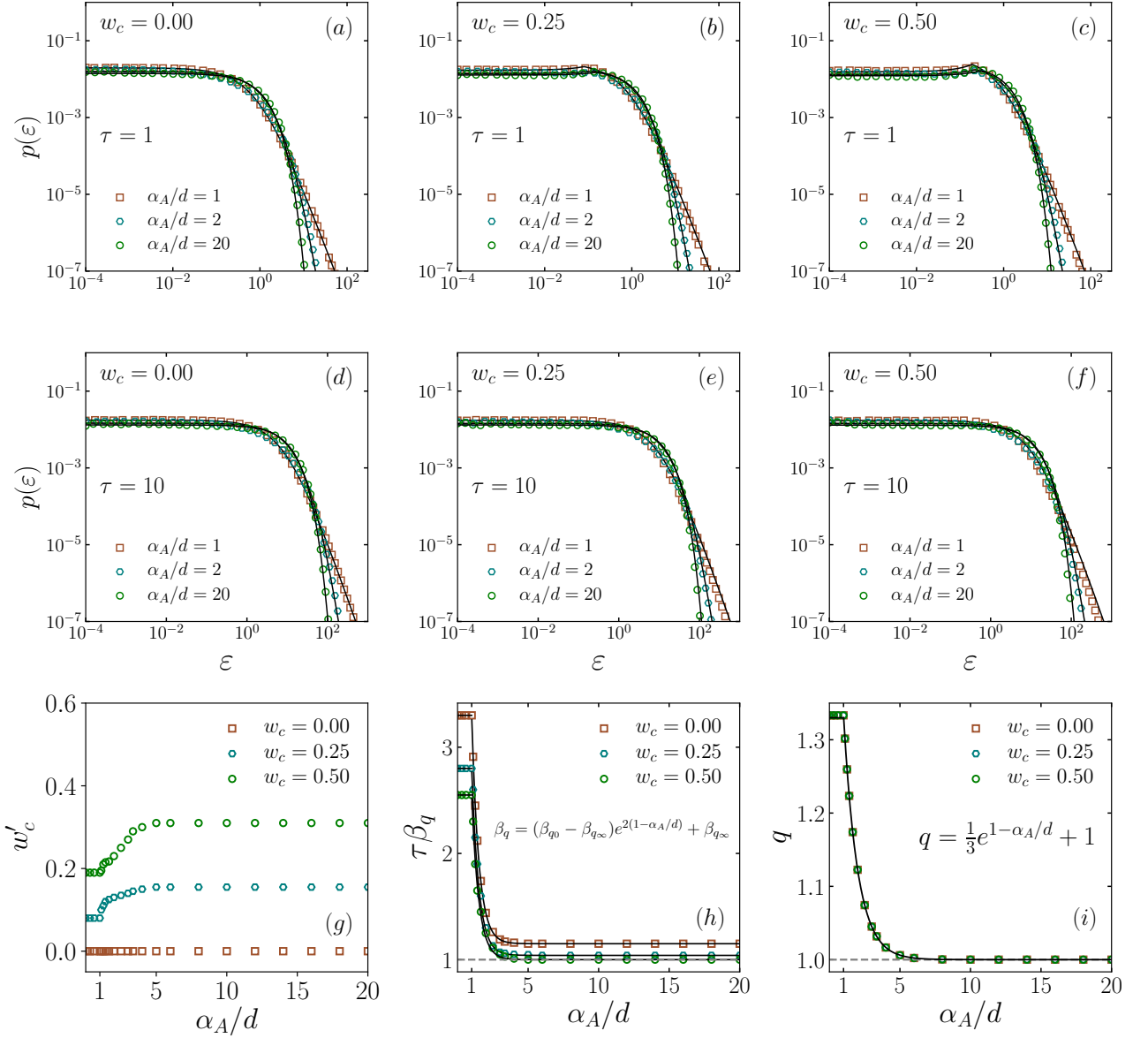


FIG. 7. *Top:* Energy distribution for  $w_c = 0.00$  (a),  $w_c = 0.25$  (b) and  $w_c = 0.50$  (c), and  $\alpha_A/d = 1, 2, 20$ , with  $\tau = 1$ . The plots (d)-(f) are the same as in (a)-(c) but with  $\tau = 10$ . The black continuous lines correspond to Eq. (7) with  $q$  and  $\beta_q$  given by Eqs. (8) and (9) respectively. *Bottom:* (d)  $w'_c$  as function of  $\alpha_A/d$  for typical values of  $w_c$ ;  $w'_c$  is constant for  $0 \leq \alpha_A/d \leq 1$ , increases for  $1 < \alpha_A/d \lesssim 5$ , and attains a constant limit for  $\alpha_A/d \rightarrow \infty$ . (e)  $\tau\beta_q$  as function of  $\alpha_A/d$  for typical values of  $w_c$ , the black continuous lines correspond to Eq. (9) with  $\beta_{q_0}$  and  $\beta_{q_\infty}$  listed in Table I. (f)  $q$  as function of  $\alpha_A/d$  and  $w_c = 0.0, 0.25, 0.5$ ; we verify that  $q = 4/3, \forall 0 \leq \alpha_A/d < 1$ , and is given by the expression which is indicated therein for  $\alpha_A/d \geq 1$ . These results remain as they stand for all values of  $\tau$ .

into a single curve for any spatial dimension. In addition to that,  $p(\varepsilon)$  does not depend on  $\alpha_G$ . We have also shown that the energy distribution  $p(\varepsilon)$  is well approached by the form  $e_q^{-\beta_q|\varepsilon-w'_c|}$ , where  $e_q^x$  is the  $q$ -exponential function emerging within  $q$ -statistics [21],  $\beta_q$  playing the role of an inverse temperature. It is quite remarkable that the  $(\alpha_A/d)$ -dependence of  $q$  precisely coincides with that obtained in [33] for a different distribution  $P(w)$ . This reinforces the strength of an universality conjecture concerning the entropic index  $q$ . In particular, Eqs. (8) and (9) appear to have a quite generic validity.

The distribution of the link weights decays exponentially. It is therefore interesting to observe that, in sensible contrast, the cooperative effect of all of the links results in a power-law-decaying distribution for the energies. This



is somewhat reminiscent of the contrast between the Einstein [46] and the Debye [47] models for solids. Indeed, the low-temperature specific heat of independent quantum harmonic oscillators (first approach for optical phonons) displays an exponential behavior while the low-temperature specific heat of coupled harmonic oscillators (first approach for acoustic phonons) follows a power law. This type of cooperative phenomenon in the network has already been observed in our previous work [33]. Consequently, it is natural that we compare this result with the  $q$ -exponential function, which is a power law with an asymptotic slope equal to  $-1/(q-1)$ .

We have also shown that, in the regime of short-range interactions ( $\alpha_A/d \rightarrow \infty$ ), the energy distribution coincides with the weight distribution for a parameter class ( $\tau \rightarrow \infty$ ,  $w_c \rightarrow 0$ ). Based on the intersection of the histograms of those two distributions, and also on the quantile-quantile plot, we have provided strong numerical evidence that this is indeed so for the distribution given in Eq. (3). It might well be that this result is more general than here verified, i.e., the same result might be true for other distributions  $P(w)$ . This type of theory applies to systems similar to mobile phone call records, where the weights of the links  $w_{ij}$  are the total duration of calls (in seconds) between the users  $i$  and  $j$ . For this type of network, the weight and the energy (or strength) distributions are similar and the widths of the links are correlated with the energies of the sites [48].

Let us conclude by a rather general comment. Various examples are known where Boltzmann-Gibbs statistical mechanical systems are isomorphic to random geometrical problems. Such is the case of the Kasteleyn-Fortuin theorem [49], where the  $q_{\text{Potts}} \rightarrow 1$  limit of the  $q_{\text{Potts}}$ -state Potts ferromagnet corresponds to bond percolation. That is also the case of the de Gennes isomorphism [50], where the  $n \rightarrow 0$  limit of the  $n$ -vector ferromagnet corresponds to self-avoiding random walk, cornerstone of polymer physics. Our present numerical results suggest that analogous connections appear to exist between nonextensive statistical mechanical systems and (asymptotically) scale-free random networks.

## ACKNOWLEDGEMENTS

We thank the High Performance Computing Center (NPAD/Universidade Federal do Rio Grande do Norte) for providing computational resources. Partial financial support from CNPq, Capes and Faperj (Brazilian agencies) is acknowledged as well.

- 
- [1] Mason O and Mark V 2007 Graph theory and networks in biology *IET Syst. Biol.* **1** 89-119.
  - [2] Proulx S R, Promislow D E and Phillips P C 2005 Network thinking in ecology and evolution *Trends Ecol. Evol.* **20** 345-353.
  - [3] Wasserman S and Faust K 1994 Social Network Analysis: Methods and Applications (Cambridge: Cambridge University Press).
  - [4] Boccaletti S, Latora V, Moreno Y, Chavez M and Hwang D U 2006 Complex networks: Structure and dynamics *Phys. Rep.* **424** 175-308.
  - [5] Lind P G, da Silva L R, Andrade J J S and Herrmann H J 2007 Spreading gossip in social networks *Phys. Rev. E* **76** 036117.
  - [6] Tilch G, Ermakova T and Fabian B 2020 A multilayer graph model of the internet topology *Int. J. Netw. Virtual Organ.* **22** 219-245.
  - [7] Brito S, Canabarro A, Chaves R and Cavalcanti D 2020 Statistical properties of the quantum internet *Phys. Rev. Lett.* **124** 210501.
  - [8] Newman M E J 2001 The structure of scientific collaboration networks *Proc. Natl. Acad. Sci. USA* **98** 404-409.
  - [9] Newman M E J 2001 Scientific collaboration networks. I. Network construction and fundamental results *Phys. Rev. E* **64** 016131.
  - [10] Danon L *et al* 2011 Networks and the epidemiology of infectious disease *Interdisc. Persp. Infect. Diseases* 284909.
  - [11] Firth J A, Hellewell J, Klepac P, Kissler S, Kucharski A J and Spurgin L G 2020 Using a real-world network to model localized covid-19 control strategies *Nat. Med. (N. Y., U. S.)* **26** 1616-1622.
  - [12] Sporns O, Tononi G, Kötter R 2005 The Human Connectome: A Structural Description of the Human Brain *PLoS Comput Biol* **1(4)**: e42.
  - [13] Newman M E J 2003 The structure and function of complex networks *SIAM Rev.* **45** 167-256.
  - [14] Latora V and Marchiori M 2002 Is the Boston subway a small-world network? *Physica A* **314** 109-113.
  - [15] Sporns O 2003 Network analysis, complexity, and brain function *Complexity* **8** 56-60.
  - [16] Gastner M T and Newman M E 2006 The spatial structure of networks *Eur. Phys. J. B* **49** 247-252.
  - [17] Newman M E J 2004 Analysis of weighted networks *Phys. Rev. E* **70** 056131.
  - [18] Allard A, Serrano M, García-Pérez G, and Boguñá M 2017 The geometric nature of weights in real complex networks *Nat. Commun* **8** 14103.

- [19] Cheung D P and Gunes M H 2012 In *IEEE/ACM International Conference on Advances in Social Networks Analysis and Mining* 699-701.
- [20] Campa A, Dauxois T, Fanelli D and Ruffo S 2014 *Physics of Long-Range Interacting Systems* (Oxford: Oxford University Press).
- [21] Tsallis C 1988 Possible generalization of Boltzmann–Gibbs statistics *J. Stat. Phys.* **52** 479–87.
- [22] Pickup R M, Cywinski R, Pappas C, Farago B and Fouquet P 2009 Generalized spin-glass relaxation *Phys. Rev. Lett* **102**, 097202.
- [23] Livadiotis G and McComas D J 2011 Invariant kappa distribution in space plasmas out of equilibrium *Astrophys. J.* **741** 88.
- [24] Malacarne L C, Mendes R S and Lenzi E K 2001 q-Exponential distribution in urban agglomeration *Phys. Rev. E* **65** 017106.
- [25] Lin S Z *et al* 2020 Universal statistical laws for the velocities of collective migrating cells *Adv. Biosys.* **4** 2000065.
- [26] Douglas P, Bergamini S and Renzoni F 2006 Tunable Tsallis distributions in dissipative optical lattices *Phys. Rev. Lett.* **96** 110601.
- [27] Lutz E and Renzoni F 2013 Beyond Boltzmann–Gibbs statistical mechanics in optical lattices *Nat. Phys.* **9** 615–619.
- [28] Soares D J, Tsallis C, Mariz A M and da Silva L R 2005 Preferential attachment growth model and nonextensive statistical mechanics *Europhys. Lett.* **70** 70.
- [29] Brito S, da Silva L R and Tsallis C 2016 Role of dimensionality in complex networks *Sci. Rep.* **6** 27992.
- [30] Nunes T C, Brito S, da Silva L R and Tsallis C 2017 Role of dimensionality in preferential attachment growth in the Bianconi–Barabási model *J. Stat. Mech.* **(2017)** 093402.
- [31] Brito S, Nunes T C, da Silva L R and Tsallis C 2019 Scaling properties of  $d$ -dimensional complex networks *Phys. Rev. E* **99** 012305.
- [32] Cinardi N, Rapisarda A and Tsallis C 2020 A generalised model for asymptotically-scale-free geographical networks *J. Stat. Mech.* 043404.
- [33] de Oliveira R M, Brito S, da Silva L R and Tsallis C 2021 Connecting complex networks to nonadditive entropies *Sci. Rep.* **11** 1130.
- [34] Thas O 2010 *Comparing Distributions* (New York: Springer).
- [35] Young I 1977 Proof without prejudice: use of the Kolmogorov-Smirnov test for the analysis of histograms from flow systems and other sources *J. Histochem. Cytochem.* **25** 935-941.
- [36] Peacock J A 1983 Two-dimensional goodness-of-fit testing in astronomy *Mon. Not. R. Astron. Soc.* **202** 615–627.
- [37] Swain M J and Ballard D H 1991 Color indexing *IJCV* **7** 11–32.
- [38] Yang M H, Kriegman D J and Ahuja N 2002 Detecting faces in images: A survey *IEEE Trans. Pattern Anal. Mach. Intell.* **24** 34-58.
- [39] Wiesebron L E, Horne J K, Scott B E and Williamson B J 2016 Comparing nekton distributions at two tidal energy sites suggests potential for generic environmental monitoring *Int. J. Mar. Energy* **16** 235-249.
- [40] Yook S H, Jeong H, Barabási A L and Tu Y 2001 *Phys. Rev. Lett.* **86** 5835.
- [41] Wang S and Zhang C 2004 Weighted competition scale-free network *Phys. Rev. E* **70** 066127.
- [42] Barthelemy M, Barrat A, Pastor-Satorras R and Vespignani A 2005 Characterization and modeling of weighted networks *Physica A* **346** 34-43.
- [43] Devroye L 1986 *Non-uniform random variate generation* (New York: Springer-Verlag).
- [44] Harris C R *et al* 2020 Array programming with NumPy *Nature* **585** 357-362.
- [45] Serfling R J 1980 *Approximation Theorems of Mathematical Statistics* (New York: Wiley).
- [46] Ashcroft, N. W. and Mermin, N. D. 1976 *Solid State Physics* (Philadelphia, PA: Holt Saunders).
- [47] Debye, P. 1912 Zur theorie der spezifischen wärmen *Annalen der Physik* **344(14)** 789-839.
- [48] Onnela, Jukka-Pekka, et al. 2007 Analysis of a large-scale weighted network of one-to-one human communication *New J. Phys.* **9** 179.
- [49] Kasteleyn P. W. and Fortuin C. M. 1969 Phase transitions in lattice systems with random local properties *J. Phys. Soc. Jpn.* **26** 11.
- [50] de Gennes P G 1972 Exponents for the excluded volume problem as derived by the Wilson method *Phys. Lett. A* **38** 339.